Identification of the Hydrophobic Thickness of a Membrane Protein Using Fluorescence Spectroscopy: Studies with the Mechanosensitive Channel MscL[†,1]

Andrew M. Powl, J. Neville Wright, J. Malcolm East, and Anthony G. Lee*

School of Biological Sciences, University of Southampton, Southampton SO16 7PX, U.K.

Received December 20, 2004; Revised Manuscript Received February 3, 2005

ABSTRACT: The hydrophobic thickness of a membrane protein is an important parameter, defining how the protein sits within the hydrocarbon core of the lipid bilayer that surrounds it in a membrane. Here we show that Trp scanning mutagenesis combined with fluorescence spectroscopy can be used to define the hydrophobic thickness of a membrane protein. The mechanosensitive channel of large conductance (MscL) contains two transmembrane α-helices, of which the second (TM2) is lipid-exposed. The region of TM2 that spans the hydrocarbon core of the bilayer when MscL is reconstituted into bilayers of dioleoylphosphatidylcholine runs from Leu-69 to Leu-92, giving a hydrophobic thickness of ca. 25 Å. The results obtained using Trp scanning mutagenesis were confirmed using Cys residues labeled with the *N*-methylamino-7-nitroben-2-oxa-1,3-diazole [NBD] group; both fluorescence emission maxima and fluorescence lifetimes for the NBD group are sensitive to solvent dielectric constant over the range (2−40) thought to span the lipid headgroup region of a lipid bilayer. Changing phospholipid fatty acyl chain lengths from C14 and C24 results in no significant change for the fluorescence of the interfacial residues, suggesting very efficient hydrophobic matching between the protein and the surrounding lipid bilayer.

Integral membrane proteins are shaped, in part, by interaction with the surrounding lipid bilayer (*1*); lipids and proteins must therefore have coevolved to give functional membrane systems. One obviously important property of a lipid bilayer is its hydrophobic thickness, defined, for a bilayer of a glycerophospholipid, as the distance between the glycerol backbone regions of the lipid molecules on the two sides of the bilayer. The hydrophobic thickness of a membrane protein can be expected to match that of the surrounding lipid bilayer, because the cost of exposing hydrophobic groups to water is high (*2*); mismatch between the hydrophobic thicknesses can lead to loss of activity, presumably as a result of distortion of the protein (*3*). The hydrophobic thickness of a membrane protein can be determined directly from the crystal structure in those few cases where the crystal structure contains several resolved lipid molecules (*3*). However, crystal structures of most integral membrane proteins do not include resolved lipid molecules and the hydrophobic thickness of the protein has then to be deduced indirectly. Complications arise from the facts that transmembrane α-helices often extend beyond the likely position of the lipid bilayer, that transmembrane α-helices usually have to span the lipid headgroup region as well as the hydrophobic core of the bilayer, and that the ends of transmembrane α-helices may not be well defined because of the need to provide suitable hydrogen bonding partners for residues at the ends of the helices

Here we develop two experimental approaches to determining the hydrophobic thickness of a membrane protein. The first makes use of the environmental sensitivity of Trp fluorescence emission (*4*) to identify the location, within a lipid bilayer, of Trp residues introduced into the lipid-exposed face of a transmembrane α-helix. In particular, experiments with the potassium channel KcsA (*5*), which contains five Trp residues per monomer, all at the ends of transmembrane α-helices, have identified the wavelength of maximum fluorescence emission for a Trp residue located immediately below the glycerol region of a lipid bilayer (332.6 nm on the instrument used here), allowing the identification of the ends of the hydrocarbon core-spanning region of a transmembrane α-helix.

The method requires that introduction of a Trp residue into the protein does not change significantly the structure of the protein or its interaction with the lipid bilayer. It has been suggested that, since Trp residues are found preferentially at the ends of transmembrane α-helices (*6*, *7*), Trp residues could play a special role in anchoring transmembrane α-helices into the surrounding lipid bilayer, although the force of this argument is weakened by the fact that Trp residues at the ends of transmembrane α-helices are generally not conserved. The preference of Trp residues for the membrane interface has been shown in glycosylation mapping experiments by Braun and von Heijne (*8*). In these experiments, the second transmembrane α-helix of leader peptidase was replaced by a stretch of Leu residues and it was shown that introduction of a Trp residue into the C-terminal end of the second helix led to a significant repositioning of the helix (*8*). These results contrast with

[†] We thank the BBSRC for financial support and for a studentship (to A.M.P.).

* To whom correspondence should be addressed. Phone: 44 (0) 2380 594331. Fax: 44 (0) 2380 594459. E-mail: agl@soton.ac.uk.

[1] Abbreviations: MscL, mechanosensitive channel of large conductance; di(C12:0)PC, didodecylphosphatidylcholine; di(C14:1)PC, dimyristoleoylphosphatidylcholine; di(C18:1)PC, dioleoylphosphatidylcholine; di(C24:1)PC, dinervonylphosphatidylcholine; di(Br_2C18:0)PC, di(9,10-dibromostearoyl)phosphatidylcholine; IANBD, *N*-((2-(iodoacetoxy)ethyl)-*N*-methyl)amino-7-nitrobenz-2-oxa-1,3-diazole; IPTG, isopropyl-β-D-thiogalactopyranoside.

10.1021/bi047338g CCC: $30.25
Published on Web 03/25/2005

fluorescence experiments by Ren et al. (*9*) with Lys-flanked poly-Leu helices in lipid bilayers which showed that Trp residues introduced into the helices occupied depths in the lipid bilayer linearly related to their position in the amino acid sequence, providing no evidence that introduction of a Trp residue into the helix led to a change in the position of the helix within the bilayer. A key difference between the two sets of experiments could be that in the experiments of Braun and von Heijne (*8*) there were no charged residues at the C-terminal end of the second transmembrane α-helix able to anchor the helix firmly into the membrane; the Trp residue, when introduced into the C-terminal end, could then play this anchoring role with no competition from other residues. This is consistent with experiments with diacylglycerol kinase, which suggest that the presence of Trp residues is redundant when transmembrane α-helices are anchored into the membrane by charged groups; the major role of the Trp residues appeared to be to increase the thermal stability of the protein (*10*). A further important factor to be considered in a multihelix membrane protein is that the energetics of shifting the location of one transmembrane α-helix will be affected by interactions between that helix and the other helices in the protein, by effects on the structure of the loops at the N- and C-terminal ends of the helix, and by effects of loop−loop interactions. In the experiments of Braun and von Heijne (*8*) the second transmembrane α-helix in leader peptidase was deliberately replaced by a stretch of Leu residues in order to remove any specific interactions with the first transmembrane α-helix that might restrict movement of the second helix.

It has been shown experimentally that multihelix membrane proteins are, in fact, well able to accommodate the introduction of Trp residues. For example, it has been shown for the *Shaker* potassium channel that introduction of Trp residues into 21 out of 22 positions in transmembrane α-helix S1, into 22 out of 23 positions in S2, and into all 22 positions tested in S3 gave functional channels (*11*, *12*). On the basis of these experiments, Monks et al. (*11*) concluded that Trp residues were relatively nonperturbing in transmembrane α-helices, particularly on the face of the helix predicted to be lipid-exposed. The only locations in the transmembrane α-helices of the *Shaker* potassium channel where the introduction of Trp residues prevented the correct folding of the protein were at locations of high conservation, likely to be involved in protein−protein contact (*11*, *12*). These results are consistent with the observation that all but 7 residues in diacylglycerol kinase could be substituted with retention of some activity (*13*), although mutations at a larger number of sites can lead to loss of stability (*14*).

The second fluorescence method used here makes use of the environmental sensitivity of the fluorescence of Cys residues labeled with *N*-((2-(iodoacetoxy)ethyl)-*N*-methyl)-amino-7-nitrobenz-2-oxa-1,3-diazole [IANBD]. Because of the polarity of the NBD group, the NBD group has a tendency to locate at the lipid−water interface, as shown by experiments with phospholipids containing NBD-labeled fatty acyl chains (*15*). In this, therefore, the fluorescent NBD group should be similar to the polar methanesulfonate spin labels used to label Cys residues in proteins for electron spin resonance studies of membrane protein structure (*16*).

The membrane protein studied here is the mechanosensitive channel of large conductance (MscL) from *Mycobacterium tuberculosis*; the protein contains no Trp or Cys residues. The crystal structure of MscL from *M. tuberculosis*, determined at a resolution of 3.5 Å (*17*), shows the channel to be a homopentamer, each monomer containing two transmembrane α-helices, the second of which (TM2) is lipid-exposed (Figure 1). The periplasmic end of TM2 is well defined by the position of Asp-68, but the cytoplasmic end is not defined by the presence of charged residues. Tyr residues are often found at the ends of transmembrane α-helices (*7*); Tyr residues located at positions 87 and 94 at the cytoplasmic end of TM2 would, if marking the cytoplasmic end of TM2, define hydrophobic thicknesses for MscL of ca. 20 and 34 Å, respectively (Figure 1). Neither of these estimates would be in good agreement with the estimated hydrophobic thickness of 24 Å derived from the observation that the phosphatidylcholine showing strongest binding to MscL has a chain length of C16, a chain length that would produce a liquid crystalline bilayer with a hydrophobic thickness of 24 Å (*18*).

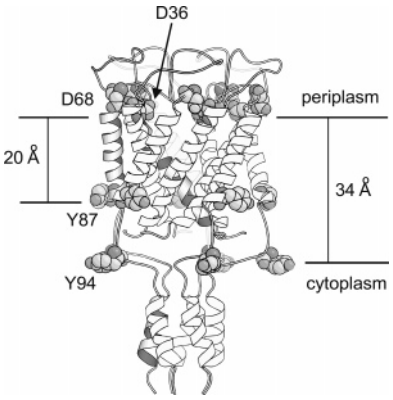

FIGURE 1: Structure of MscL. Possible locations for the hydrophobic domain on MscL are shown, defined by the positions of Asp-36 and Asp-68 on the periplasmic side of the membrane and either Tyr-87 or Tyr-94 on the cytoplasmic side. The figure was prepared using Bobscript (*38*) and the coordinates in PDB IMSL.

MscL opens on increasing tension in the membrane, and because MscL is fully functional when reconstituted alone into lipid vesicles, membrane tension must be transduced directly from the lipid molecules to the protein (*19*, *20*). Interaction between the lipid bilayer and the protein is therefore particularly important for MscL. It has been shown that the applied pressure required to open MscL decreases with decreasing bilayer thickness, consistent with a decrease in hydrophobic thickness for MscL on channel opening (*21*). We show here that fluorescence spectroscopy can also be used to study how changing bilayer thickness affects the way that MscL sits in a lipid bilayer. Trp and Cys residues were introduced into nonconserved regions of the MscL structure, externally facing residues not involved in helix−helix interactions (Figure 2) being chosen to minimize the chances of structural perturbation by the introduced residues.

MATERIALS AND METHODS

Protein Expression and Purification. A plasmid containing the *M. tuberculosis mscL* gene with a poly-His epitope at the N-termini was the generous gift of Professor D. C. Rees. Site directed mutagenesis was performed using the Quickchange protocol from Stratagene. The fidelity of the products

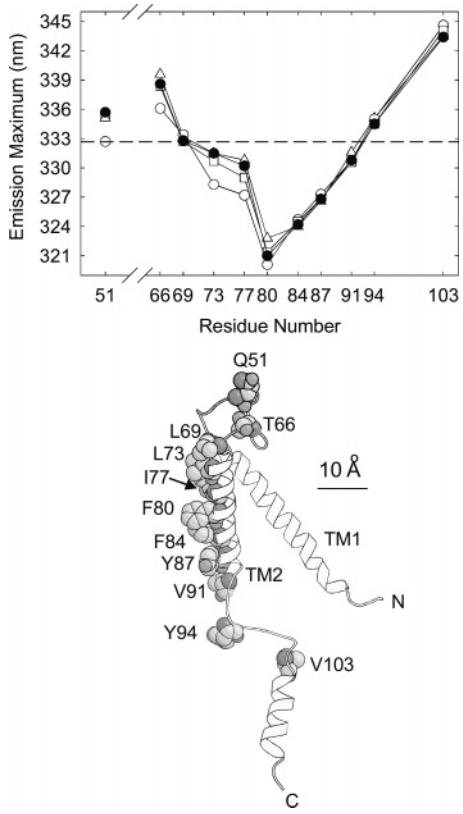

FIGURE 2: Fluorescence properties of Trp mutants of MscL. Trp fluorescence emission maxima (nm) for Trp mutants are plotted as a function of position, for MscL reconstituted in (○) di(C12:0)PC, (□) di(C14:1)PC, (●) di(C18:1)PC, and (△) di(C24:1)PC. The dotted line at 332.6 nm marks the expected fluorescence emission maximum for a Trp residue immediately below the glycerol backbone region of the bilayer. The lower panel shows the locations of the mutated residues in MscL.

was confirmed by sequence analysis. *Escherichia coli* BL21-(DE3)pLysS transformants carrying the pET-19b plasmid (Novagen) with the *mscL* gene were grown in 6 L of Luria broth to mid-log phase ($OD_{600} = 0.6$) and then induced for 3 h in the presence of isopropyl-β-D-thiogalactopyranoside [IPTG] (1.0 mM). MscL was purified as described in Powl et al. (*18*).

In Vivo Channel Function Assay. Loss of function mutants were detected by measuring the ability of MscL mutants to rescue *E. coli* strain MJF465 lacking mechanosensitive channels (*22*) from the effects of osmotic downshock, as described in Powl et al. (*18*). *E. coli* MJF465 transformants carrying the pET-19b plasmid with the MscL gene were grown in 10 mL of Luira broth containing ampicillin (100 μg/mL) supplemented with 0.4 M NaCl. Cells were grown for 16 h at 37 °C in an orbital shaker and used to seed fresh cultures (10 mL) that were grown in the presence of IPTG for 4 h. Cells were harvested by centrifugation and the cell pellet was resuspended in sterile 0.4 M NaCl to produce a concentration of cells equivalent to an apparent absorbance at 600 nm of 5. Cell suspensions (30 μL) were then diluted 60-fold into either 0.4 M NaCl or distilled water, both containing ethidium bromide (0.5 μg/mL). Cells were incubated for 45 min at room temperature followed by pelleting. The supernatant was assayed for the release of DNA, measuring the fluorescence intensity at 632 nm, with excitation at 254 nm.

Gain of function mutants were detected by a reduced rate of growth after induction of MscL production with IPTG (*23*).

Lipids and Reconstitution. Didodecylphosphatidylcholine [di(C12:0)PC], dimyristoleoylphosphatidylcholine [di(C14:1)PC], dioleoylphosphatidylcholine [di(C18:1)PC], and dinervonylphosphatidylcholine [di(C24:1)PC] were obtained from Avanti Polar Lipids. Di(9,10-dibromostearoyl)-phosphatidylcholine (di(Br_2C18:0)PC) was prepared by bromination of di(C18:1)PC as described in East and Lee (*24*).

Purified MscL was reconstituted into lipid bilayers by mixing lipid and MscL in cholate, followed by dilution into buffer to decrease the concentration of cholate below its critical micelle concentration, as described (*18*). This procedure produces unsealed membrane fragments (see ref *25*), allowing ready access to both sides of the membrane.

Labeling of MscL. Cys-containing mutants of MscL were labeled with IANBD by incubating MscL (225 μM) with IANBD (3.6 mM) in PBS buffer (350 μL; 140 mM NaCl, 2.7 mM KCl, 10 mM Na_2HPO_4, 1.8 mM KH_2PO_4, pH 7.2) containing tri(2-carboxyethyl)phosphine hydrochloride (3 mM) for 1.5 h at 25 °C, followed by removal of unreacted label on a G-25 Sepharose column. Nanoelectrospray mass spectrometry (LCT orthogonal acceleration-TOF instrument, Micromass) was used to confirm a 1:1 molar ratio of labeling of MscL by IANBD.

Fluorescence Measurements. Trp fluorescence was recorded for 0.98 μM MscL in buffer (20 mM Hepes, 100 mM KCl, 1 mM EGTA, pH 7.2) at 25 °C, using an SLM 8100 fluorimeter, generally with excitation at 280 nm. Background corrections were made by subtraction of a spectrum recorded for lipid samples alone in buffer; at the lipid concentrations used here, typically 100 μM, light scatter caused no distortion of the spectra of the type observed by Ladokhin et al. (*26*) at high lipid concentrations. Spectra were corrected for the wavelength dependence of instrumental sensitivity using a set of correction factors generated by comparison of an emission spectrum for tryptophan in buffer with the corrected emission spectrum for tryptophan published by Chen (*27*). To obtain accurate values for wavelengths of maximum fluorescence emission, intensity corrected fluorescence spectra were fitted to skewed Gaussian curves (*10*). The emission maximum for a solution of indole in ethanol was 322.8 nm on the fluorimeter used for these studies. Fluorescence of NBD-labeled MscL was recorded for 0.6 μM MscL with excitation at 478 nm.

In quenching experiments with acrylamide and iodide, the inner filter effect was minimized by exciting fluorescence at 295 nm, corrections for the inner filter effect being made by applying the correction factor $10^{0.5c\epsilon}$, where ϵ is the molar extinction coefficient at 295 nm and c is the concentration of quencher. Acrylamide was added from a 1 M stock solution in buffer. For quenching studies with iodide, a stock solution of 1 M KI in buffer containing 100 mM $Na_2S_2O_3$ was added to MscL (0.98 μM) in buffer containing KCl at a concentration chosen to maintain the total concentration KI + KCl at 0.91 M. In quenching studies with 1,2-diiodobenzene, the required amount of 1,2-diiodobenzene was mixed with lipid in chloroform, and the mixture was dried down and then resuspended in cholate-containing buffer for reconstitution with MscL, as described above.

Table 1: Fluorescence Peak Width for Trp Mutants of MscL Reconstituted with Phosphatidylcholines[a]

	peak width ω (nm)			
mutant	di(C12:0)PC	di(C14:1)PC	di(C18:1)PC	di(C24:1)PC
Q51W	60.7 ± 0.2	56.7 ± 0.2	57.2 ± 0.2	56.9 ± 0.2
T66W	67.8 ± 0.4	60.8 ± 0.4	61.5 ± 0.3	61.0 ± 0.3
L69W	62.7 ± 0.4	53.0 ± 0.1	53.1 ± 0.1	53.4 ± 0.2
L73W	51.5 ± 0.2	52.9 ± 0.2	53.7 ± 0.2	53.4 ± 0.2
I77W	51.7 ± 0.2	50.8 ± 0.1	51.9 ± 0.1	51.7 ± 0.2
F80W	42.9 ± 0.2	46.3 ± 0.1	44.1 ± 0.2	45.8 ± 0.3
F84W	47.0 ± 0.1	46.0 ± 0.2	47.0 ± 0.1	47.0 ± 0.1
Y87W	46.9 ± 0.1	46.4 ± 0.1	47.1 ± 0.1	49.0 ± 0.2
V91W	49.2 ± 0.1	49.4 ± 0.1	50.0 ± 0.1	51.7 ± 0.2
Y94W	52.8 ± 0.1	52.1 ± 0.1	52.7 ± 0.1	53.8 ± 0.1
V103W	62.6 ± 0.3	59.6 ± 0.2	59.4 ± 0.2	59.7 ± 0.3

[a] ω is the peak width at half-height determined by fitting intensity corrected fluorescence emission spectra to the equation for a skewed Gaussian (*10*).

Fluorescence lifetimes were recorded using a PTI GL-3300 lifetime fluorimeter equipped with a PTI nitrogen dye laser, with excitation at 478 nm, at a concentration of MscL of between 0.2 and 2.0 μM. Fluorescence decays were fitted to sums of two and three exponentials, and the average lifetime was calculated as described by Lakowicz (*4*).

RESULTS

In Vivo Channel Function Assay. In vivo phenotype assays have been developed to test for MscL mutations causing loss or gain of function (*28*). To test for loss of function mutants, mutant MscLs were expressed in *E. coli* strain MJF465 lacking mechanosensitive channels, making them sensitive to osmotic downshock (*22*). Functional MscL mutants are able to rescue the *E. coli* cells from the effects of osmotic downshock, as shown using a fluorescence assay to measure levels of release of DNA. Gain of function mutants are detected by a reduced rate of growth after induction of MscL production with IPTG (*23*). None of the mutations studied here resulted in loss of function mutations, and any effects of the mutations on growth rate were small, showing that the mutations also did not create any gain of function mutations. Although these assays for function would not be able to detect any subtle changes in protein function, the lack of gain of function mutants show that, in the absence of an applied tension, all the mutant channels will be in the closed state.

The Use of Trp Mutants To Locate the Hydrophobic Surface of MscL. Residues on the lipid-exposed face of the second transmembrane α-helix (TM2), together with a number of solvent-exposed flanking residues, were mutated to Trp (Figure 2). Fluorescence emission maxima were determined for the resulting protein reconstituted into bilayers of di(C18:1)PC (Figure 2). The emission width at half-height varied from ca. 44 nm for F80W to ca. 60 nm for T66W and V103W (Table 1). These results are consistent with the relationship between fluorescence emission maximum and peak width established by Ladokhin et al. (*26*), showing that the Trp-containing MscLs adopt a single conformational state in di(C18:1)PC, since a mixture of conformational states would have led to a greater than expected width for the fluorescence emission peak.

The Trp emission maximum of 322.0 nm for F80W (Figure 2) is comparable to that for the Trp residue in

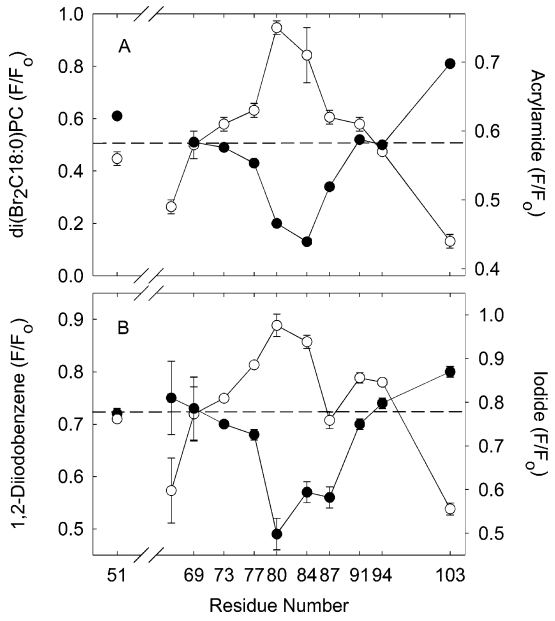

FIGURE 3: Fluorescence quenching of Trp mutants of MscL. Values of F/F_0 are plotted as a function of Trp position, where F_0 and F are fluorescence intensities in the absence and presence of quencher, respectively. (A) (●) MscL reconstituted in di(Br_2C18:0)PC. (○) MscL reconstituted in di(C18:1)PC in the presence of 0.25 M acrylamide. (B) (●) MscL reconstituted in di(C18:1)PC in the presence of 45 μM 1,2-diiodobenzene. (○) MscL reconstituted in di(C18:1)PC in the presence of 0.45 M iodide. In A and B the dotted lines have been drawn through the points for L69W. The concentration of MscL monomer was 0.98 μM, and the molar ratio of lipid to MscL monomer was 100:1.

the peptide Ac-KL_7WL_9KA-amide reconstituted into di(C18:1)PC (λ_{max} of 318 nm), consistent with a location for the Trp residue in F80W close to the middle of the bilayer. Trp emission maxima move to longer wavelengths with increasing distance from position 80 (Figure 2). Studies with the potassium channel KcsA reconstituted into bilayers of di(C18:1)PC suggest that a Trp residue located immediately below the glycerol backbone region of a lipid bilayer will emit at 332.6 nm (*5*), locating the interfacial residues as Leu-69 on the lumenal side of the membrane and a residue between Val-91 and Tyr-94 on the cytoplasmic side (Figure 2).

Identification of the interfacial residues was confirmed by fluorescence quenching studies. Trp fluorescence is quenched by phospholipids containing dibrominated fatty acyl chains, the efficiency of quenching depending on the sixth power of the distance between the Trp and the dibromo group (*18*, *29*). This could indicate either that fluorescence quenching was by a Forster energy transfer mechanism with a value for R_o, the distance at which energy transfer is 50% efficient, of 8 Å (*18*) or that quenching was collisional, taking into account the depth distribution of the fluorophore and quencher in the membrane (*30*). The highest level of quenching in bilayers of di(Br_2C18:0)PC, in which the dibromo group is located at the 9 and 10 positions in the fatty acyl chains, is observed for F84W, the level of quenching decreasing for Trp residues further from this position, quenching of L69W being equal to that of V91W and Y94W on the cytoplasmic side (Figure 3A). The fact that significant quenching is observed for Q51W, T66W, and V103W, three residues located in region of the protein

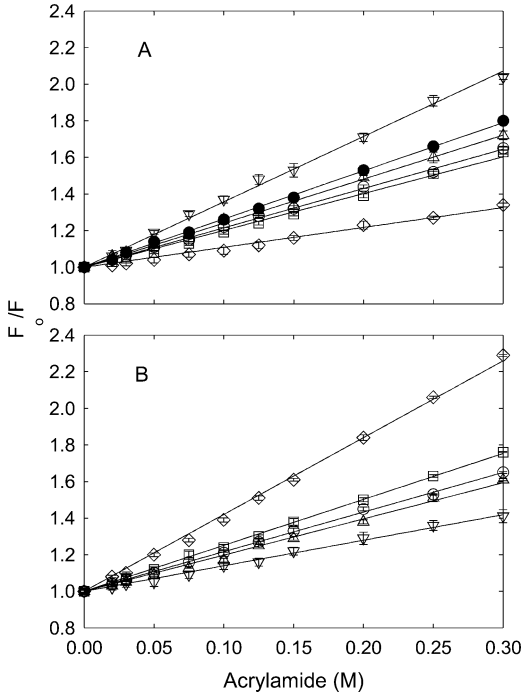

FIGURE 4: Stern−Volmer plots for quenching of the Trp fluorescence of MscL by acrylamide. Trp mutants of MscL were reconstituted into bilayers of di(C18:1)PC. Fluorescence intensities are expressed as the ratio F_0/F where F_0 and F are the intensities in the absence and presence of acrylamide, respectively. Trp mutants are as follows: (A) (●) Q51W, (▽) T66W, (△) L69W, (○) L73W, (□) I77W, and (◇) F80W; (B) (▽) F84W, (△) Y87W, (○) V91W, (□) Y94W, and (◇) V103W. The solid lines show fits to eq 1, giving the values for K_{SV} listed in Table 4. The concentration of MscL was 0.98 μM, and the molar ratio of lipid to MscL was 100:1. Data points are the average of three determinations and corrected for the inner-filter effect.

outside the hydrophobic core of the lipid bilayer, is consistent with a Forster energy transfer mechanism for quenching.

Quenching of Trp fluorescence in the MscL mutants by the water soluble quencher acrylamide fits the Stern−Volmer equation

$$F_0/F = 1 + K_{SV}[Q] \quad (1)$$

for all the mutants, where F_0 and F are fluorescence intensities in the absence and presence of quencher Q, respectively, and K_{SV} is the Stern−Volmer quenching constant (Figure 4). Caputo and London (*31*) have shown that acrylamide quenching of the Trp fluorescence of Trp-containing peptides incorporated into lipid bilayers also fits to the Stern−Volmer equation, the level of quenching being inversely related to the distance of the Trp residue from the center of the bilayer. Caputo and London (*31*) report levels of quenching of Trp-containing peptides by 235 mM acrylamide. For comparison, Figure 3A shows levels of fluorescence quenching of the Trp-containing mutants of MscL in di(C18:1)PC by 250 mM acrylamide. The profile of quenching is the inverse of that seen with di(Br_2C18:0)PC, the lowest level of quenching being observed for F80W (Figure 3A). The 42% quenching observed for L69W with 0.25 M acrylamide compares to the ca. 40% quenching by 0.24 M acrylamide for Trp residues at the ends of a model transmembrane α-helix in a lipid bilayer (*31*), and the 37% quenching observed for the Trp residues in KcsA (*10*). The

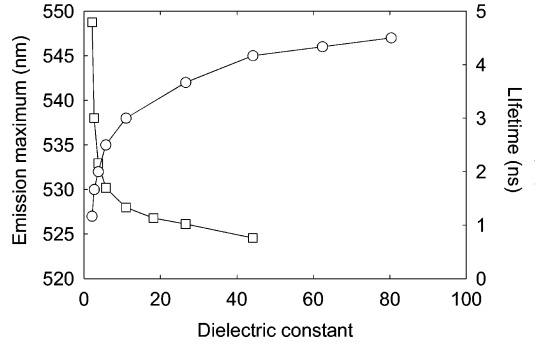

FIGURE 5: Fluorescence properties of IANBD in dioxane/water mixtures. Fluorescence emission maxima (○) and average fluorescence lifetimes (□) are plotted against dielectric constants for dioxane/water mixtures taken from ref *38*.

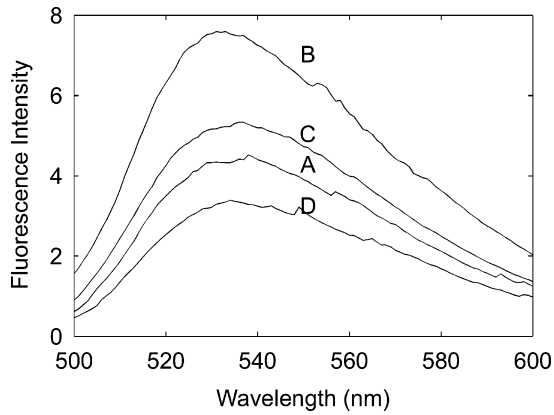

FIGURE 6: Fluorescence emission spectra of NBD-labeled Cys mutants of MscL in bilayers of di(C18:1)PC. Fluorescence emission spectra are shown for (A) NBD-L69C, (B) NBD-Y87C, (C) NBD-V91C, and (D) NBD-Y94C. The concentration of MscL was 0.6 μM, and the molar ratio of lipid to MscL was 100:1. The excitation wavelength was 478 nm, and the buffer was 20 mM Hepes, 100 mM KCl, 1 mM EGTA, pH 7.2.

level of quenching for L69W lies between the levels of quenching for V91W and Y94W (Figure 3A).

Quenching by the water-soluble iodide ion also fits to the Stern−Volmer equation (data not shown). Figure 3B shows the level of quenching caused by 0.45 M KI; the profile is more complex than that seen with the other quenchers, but quenching is again low for F80W, with a marked increase in quenching between L69W and T66W and between V91W and V103W (Figure 3B), consistent with Leu-69 and Val-91 being close to the interface. Quenching by the lipid-soluble quencher 1,2-diiodobenzene shows a profile similar to that seen with di(Br_2C18:0)PC, with the level of quenching of L69W being between that for V91W and Y94W (Figure 3B).

The Use of NBD-Labeled MscL To Locate the Hydrophobic Surface. The results obtained with the Trp mutants of MscL were confirmed using mutants containing Cys residues introduced at the ends of TM2 and labeled with IANBD. The fluorescence emission of the NBD group is sensitive to solvent polarity (*4*). Both the fluorescence emission maximum and the fluorescence lifetime of the NBD group vary with dielectric constant in mixtures of dioxane/water (Figure 5), being particularly sensitive over the range 2 to 40 characteristic of the lipid headgroup region (*32*). Figure 6 shows the fluorescence emission spectra for NBD-labeled L69C, Y87C, V91C, and Y94C. Dielectric constants esti-

Table 2: Fluorescence Properties of NBD-Labeled MscL[a]

MscL mutant	emission max (nm)	dielectric constant[b]	av fluorescence lifetime (ns)	dielectric constant[c]
L69C	536.2 ± 0.13	7.4	2.86 ± 0.02	3.0
Y87C	534.1 ± 0.15	5.0	3.67 ± 0.10	2.5
V91C	536.1 ± 0.07	7.2	3.51 ± 0.10	2.5
Y94C	537.1 ± 0.16	8.8	2.03 ± 0.07	4.0

[a] The concentration of MscL was 0.6 μM, and the molar ratio of lipid to MscL was 100:1. The buffer was 20 mM Hepes, 100 mM KCl, 1 mM EGTA, pH 7.2. [b] Calculated from the emission maximum using the calibration curve plotted in Figure 5. [c] Calculated from the average fluorescence lifetime using the calibration curve plotted in Figure 5.

mated from the emission maxima using the calibration curve in Figure 5 are listed in Table 2. The estimated dielectric constants are consistent with locations for the labeled residues close to the interface, the dielectric constants being slightly greater than the value of 2 expected for the hydrophobic core of the bilayer but much less than the value of 80 characteristic of water. The estimated dielectric constant for L69C lies between that of V91C and Y94C, consistent with the proposal that residue 69 marks the interface on the periplasmic side of the membrane and that the interface on the cytoplasmic side lies between residues 91 and 94.

Fluorescence intensities for the labeled MscL vary significantly with location (Figure 6), and the observation that L69C has an intensity between that of V91C and Y94C is again consistent with the proposal that residue 69 is located in an environment the same as that of a residue between 91 and 94 on the opposite side of the membrane. These results were confirmed by direct measurement of fluorescence lifetimes using a nanosecond pulsed laser system (Figure 7). Experimental fluorescence decays were fitted to double or triple exponentials, and the average fluorescence lifetimes were calculated as described by Lakowicz (*4*). As shown in Figure 5, fluorescence lifetimes for the NBD group vary markedly with solvent dielectric constant. Fluorescence lifetimes for the NBD group in labeled MscL will depend on a number of factors other than just environmental dielectric constant, including structural flexibility in the neighborhood of the probe, as shown, for example, for the dansyl fluorophore in lipid bilayer systems (*33*). Nevertheless, dielectric constants estimated from the average fluorescence lifetimes are similar to those estimated from fluorescence emission maxima (Table 2), and, importantly, the dielectric constant estimated for L69C lies between those estimated for V91C and Y94C and all values are consistent with an interfacial location.

The Efficiency of Hydrophobic Matching for MscL. Fluorescence emission maxima for the Trp mutants reconstituted into bilayers of di(C12:0)PC, di(C14:1)PC, and di(C24:1)PC are very similar to those reconstituted in di(C18:1)PC (Figure 2), suggesting that there is no major conformational change with changing bilayer thickness, consistent with results obtained from spin-label experiments with *E. coli* MscL (*16*). In particular, the observation that fluorescence emission maxima for L69W, V91W, and Y94W are the same in bilayers of di(C12:0)PC, di(C14:1)PC, di(C18:1)PC, and di(C24:1)PC (Figure 2) suggests that the Trp residues maintain their locations close to the interface, despite a ca. 21 Å change in bilayer thickness. This is also consistent with studies of the fluorescence

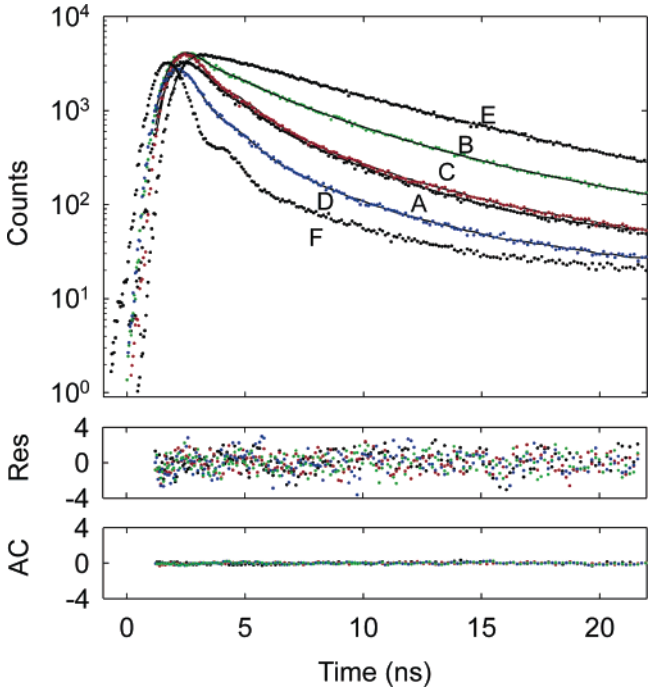

FIGURE 7: Time-resolved fluorescence decays of NBD-labeled Cys mutants of MscL in bilayers of di(C18:1)PC. Fluorescence decays are shown for (A) NBD-L69C, (B) NBD-Y87C, (C) NBD-V91C, (D) NBD-Y94C, and (E) IANBD in dioxane. The pulse profile is shown in F. The solid lines through each decay are the multiexponential fits to the data, shown as dotted lines. The lower panels show the autocorrelation and residuals for the fits. The concentration of MscL was between 0.2 and 2.0 μM, and the molar ratio of lipid to MscL was 100:1. The excitation wavelength was 478 nm, and the buffer was 20 mM Hepes, 100 mM KCl, 1 mM EGTA, pH 7.2.

Table 3: The Effect of Bilayer Thickness on Average Fluorescence Lifetimes for NBD-Labeled MscL in Bilayers of Phosphatidylcholine[a]

MscL mutant	fatty acyl chains	av fluorescence lifetime (ns)
L69C	C14:1	2.57 ± 0.04
	C24:1	2.63 ± 0.48
Y87C	C14:1	3.71 ± 0.07
	C24:1	4.06 ± 0.16
V91C	C14:1	3.51 ± 0.10
	C24:1	3.61 ± 0.36
Y94C	C14:1	2.03 ± 0.07
	C24:1	2.70 ± 0.63

[a] NBD-labeled Cys-MscL mutants were reconstituted into bilayers of phosphatidylcholines containing the given fatty acyl chains. The concentration of MscL was 0.6 μM, and the molar ratio of lipid to MscL was 100:1. The buffer was 20 mM Hepes, 100 mM KCl, 1 mM EGTA, pH 7.2.

lifetime of NBD-labeled MscL, which also show no significant changes in lifetime with bilayer thickness for any of the mutants (Table 3).

The largest shifts in Trp fluorescence emission maximum from di(C12:0)PC to di(C24:1)PC are observed for L73W and I77W (Figure 2), the 3 nm shift to longer wavelength with increasing bilayer thickness suggesting slight increases in polarity at positions 73 and 77. Since residues Leu-73 and Ile-77 are less lipid-exposed than residues such as Phe-84 and Tyr-87 (Figure 2), this could indicate a change in protein packing in the vicinity of residues 73 and 77 on changing bilayer thickness.

Table 4: Fluorescence Quenching of Trp Mutants of MscL by Acrylamide[a]

MscL mutant	F_0/F	K_{SV} (M^{-1})
Q51W	1.80 ± 0.01	2.63 ± 0.02
T66W	2.04 ± 0.01	3.57 ± 0.04
L69W	1.72 ± 0.02	2.41 ± 0.02
L73W	1.65 ± 0.01	2.15 ± 0.02
I77W	1.60 ± 0.01	2.01 ± 0.03
F80W	1.34 ± 0.01	1.09 ± 0.03
F84W	1.41 ± 0.04	1.40 ± 0.02
Y87W	1.61 ± 0.01	1.98 ± 0.03
V91W	1.65 ± 0.01	2.17 ± 0.02
Y94W	1.76 ± 0.01	2.51 ± 0.02
V103W	2.29 ± 0.01	4.20 ± 0.04

[a] F and F_0 are fluorescence intensities for MscL reconstituted in di(C18:1)PC in the presence and absence of 0.3 M acrylamide, respectively, measured at pH 7.2. The Stern−Volmer quenching constant, K_{SV}, was determined by fitting the data in Figure 4 to eq 1.

DISCUSSION

Here we show that the environmental sensitivities of the Trp and NBD groups can be used to determine which residues in a membrane protein are located at the hydrophobic-polar interfaces on the two sides of a membrane. The fact that the same conclusions are reached with both probes suggests that any perturbations of structure resulting from mutation or labeling are small. A Trp residue located immediately below the glycerol backbone region of a lipid bilayer emits at 332.6 nm on the fluorimeter used here, on the basis of studies with the potassium channel KcsA (*5*). The variation of Trp emission maxima with position (Figure 2) therefore defines the hydrophobic domain of MscL as running from Leu-69 on the periplasmic side of the membrane to a residue between Val-91 and Tyr-94 on the cytoplasmic side. This is confirmed by fluorescence emission and lifetime studies with NBD-labeled MscL (Table 2) which also show that residue 69 on the periplasmic side of the membrane is located in an environment equivalent to a residue between positions 91 and 94 on the cytoplasmic side. Fluorescence quenching results with water and lipid soluble quenchers and with di(Br_2C18:0)PC are also in agreement with these conclusions (Figure 3). In particular the level of fluorescence quenching of L69W caused by acrylamide is comparable to that seen for Trp residues at the ends of a model transmembrane α-helix in a lipid bilayer (*31*), and for the Trp residues in KcsA (*10*). The level of quenching for L69W lies between the levels of quenching for V91W and Y94W (Figure 3A).

Leu-69 is close to Asp-68, an exposed residue in MscL (Figure 8); Asp-36 is located at a distance from the bilayer center similar to that of Asp-68, but is not surface exposed (Figure 1). These results suggest that the carboxyl oxygens of Asp-68 are located close to the glycerol backbone region of the lipid bilayer. An analysis of a number of other membrane protein crystal structures suggests that this might be a common feature of membrane protein structure; for example Glu-9 in the first transmembrane α-helix of bacteriorhodopsin is close to the backbone of the neighboring lipid molecules resolved in the crystal structure (*3*).

The only charged residues on the cytoplasmic side of the membrane located at a distance from the bilayer center between those of Val-91 and Tyr-94 are Arg-11 and Asp-16 at the N-terminal end of TM1, both surface-exposed residues,

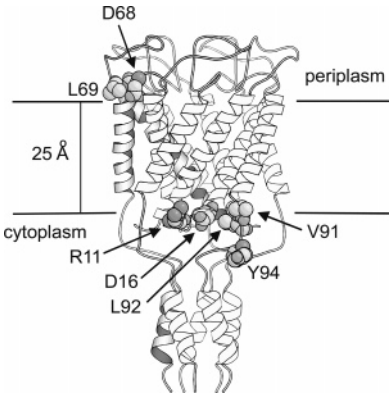

FIGURE 8: Structure of MscL with the location for the hydrophobic domain defined by fluorescence studies. The positions of Leu-69 on the periplasmic side of the membrane and of Val-91, Leu-92, and Tyr-94 on the cytoplasmic side are marked. Leu-69 is close to Asp-68 and Leu-92 to Arg-11 and Asp-16. The hydrophobic thickness of MscL, defined by the positions of Asp-68 and Asp-16, is 25 Å. One subunit of the pentamer is shown shaded. For clarity only one set of defining residues is shown: Asp-68 and Leu-69 from subunit A, Arg-11 and Asp-16 from subunit C, and Val-91, Leu-92, and Tyr-94 from subunit D. The figure was prepared using Bobscript (*37*) and the coordinates in PDB IMSL.

located close to Leu-92 in TM2 (Figure 8). The hydrophobic thickness of MscL estimated assuming that Asp-16 is located at the glycerol backbone region is ca. 25 Å (Figure 8). This agrees well with the observation that the phosphatidylcholine that binds most strongly to MscL is that with C16 chains, a chain length that gives a bilayer of hydrophobic thickness ca. 24 Å (*18*). Perozo et al. (*34*) have previously located the transmembrane region of TM2 in *E. coli* MscL as running from His-74 to Leu-98 from studies of the effects of oxygen and a water-soluble Ni^{2+} chelate on the electron spin resonance spectra of Cys mutants of MscL labeled with a methanethiosulfonate spin label. Assuming that the transmembrane region identified in the experiments of Perozo et al. (*34*) corresponds to the hydrophobic region identified here, then the hydrophobic regions of TM2 of MscL of *E. coli* and *M. tuberculosis* have very similar lengths (25 and 24 residues, respectively). This is consistent with the observation that the phosphatidylcholine that binds most strongly to *E. coli* MscL also has a chain length of C16 (*18*).

These results suggest that the region of TM2 that spans the hydrophobic core of the lipid bilayer cannot be determined by consideration of TM2 alone. Although the N-terminal end of TM2 is well marked by Asp-68, there are no charged residues close in the sequence to Leu-92 at the proposed C-terminal end of the hydrophobic core-spanning region of TM2. Although Tyr residues are often found at the ends of transmembrane α-helices (*6*, *7*), Tyr-87 and Tyr-94 in MscL (Figure 1) appear to be located either side of the interface. If, as suggested, the glycerol backbone region of the bilayer is located at a distance from the bilayer center close to Leu-92, then the hydrophobic residues in TM2 between Leu-92 and Tyr-94 would be located in the headgroup region of the bilayer, possible since the headgroup region of a bilayer of phosphatidylcholine has a thickness of about 15 Å (*1*).

It is noticeable that the plot of fluorescence emission maxima against residue number is not symmetrical about the middle of the membrane (ca. residue 80), emission

maxima for L73W and I77W being at longer wavelengths than those of Y87W and F84W, respectively (Figure 2). The structure of the MscL pentamer is such that the first and second of the transmembrane α-helices come together on the periplasmic side of the membrane (Figure 1), so that residues Phe-84 and Tyr-87 are more lipid exposed than residues Leu-77 and Ile-73. This is also apparent in molecular dynamics simulations of MscL in bilayers of phosphatidylethanolamines where lipid−residue interaction energies are stronger for residues Phe-84 and Tyr-87 than for Ile-77 and Leu-73 (*35*). A similar asymmetry is seen in fluorescence quenching plots with di(Br_2C18:0)PC and with 1,2-diiodobenzene (Figure 3), the levels of quenching of L73W and I77W being markedly less than those of F84W and Y87W, respectively, the shapes of the plots being very similar to that of the plot of emission maxima shown in Figure 2. The greater quenching observed for F84W and Y87W is consistent with greater lipid exposure of positions 84 and 87 than of positions 77 and 73. The asymmetry is less apparent in plots of quenching by the water-soluble quenchers acrylamide and iodide (Figure 3); quenching of Y87W by iodide is higher than might have been expected, which could be because Tyr-87 is located close to the positively charged guanidinium group of Arg-11.

The Efficiency of Hydrophobic Matching. The efficiency of hydrophobic matching between MscL and the surrounding lipid bilayer is high, interfacial residues maintaining their position against a 21 Å change in bilayer thickness, as seen by measurements of Trp emission maxima (Figure 2) and of NBD emission maxima and fluorescence lifetimes (Table 3). A similarly high efficiency of hydrophobic matching has been reported previously for KcsA (*5*). Presumably, hydrophobic matching is efficient because of the high cost of exposing hydrophobic surfaces, either on the protein or in the lipid bilayer, to water. It has been argued that hydrophobic matching is achieved by distortion of both the lipid bilayer and the protein (*18*), distortion of the membrane protein being a likely explanation for the decreases in activity observed for many membrane proteins in thin or thick lipid bilayers (*36*). Distortion of MscL in di(C14:1)PC is consistent with the observation that the applied pressure required to open MscL in di(C14:1)PC is less than that in di(C18:1)PC (*21*). Perozo et al. (*16*) detected significant rotation of TM1 for *E. coli* MscL on reconstitution into bilayers of di(C14:1)PC, but with no significant rotation in TM2. This is largely in agreement with the results presented here, although we did observe some small change for L73W and I77W (Figure 2), suggesting some changes at these positions in TM2 on changing bilayer thickness.

ACKNOWLEDGMENT

We thank Professor Rees for the gift of the MscL construct and Professor Booth for the gift of MJF465.

REFERENCES

1. White, S. H., Ladokhin, A. S., Jayasinghe, S., and Hristova, K. (2001) How membranes shape protein structure, *J. Biol. Chem. 276*, 32395−32398.
2. Tanford, C. (1980) *The Hydrophobic Effect: Formation of Micelles and Biological Membranes*, John Wiley, New York.
3. Lee, A. G. (2003) Lipid-protein interactions in biological membranes: a structural perspective, *Biochim. Biophys. Acta 1612*, 1−40.
4. Lakowicz, J. R.. (1999) *Principles of Fluorescence Spectroscopy*, Kluwer Academic/Plenum Press, New York.
5. Williamson, I. M., Alvis, S. J., East, J. M., and Lee, A. G. (2002) Interactions of phospholipids with the potassium channel KcsA, *Biophys. J. 83*, 2026−2038.
6. Landolt-Marticorena, C., Williams, K. A., Deber, C. M., and Reithmeier, R. A. F. (1993) Non-random distribution of amino acids in the transmembrane segments of Type 1 single span membrane proteins, *J. Mol. Biol. 229*, 602−608.
7. Ulmschneider, M. D., and Sansom, M. S. P. (2001) Amino acid distributions in integral membrane protein structures, *Biochim. Biophys. Acta 1512*, 1−14.
8. Braun, P., and von Heijne, G. (1999) The aromatic residues Trp and Phe have different effects on the positioning of a transmembrane helix in the microsomal membrane, *Biochemistry 38*, 9778−9782.
9. Ren, J. H., Lew, S., Wang, Z. W., and London, E. (1997) Transmembrane orientation of hydrophobic α-helices is regulated both by the relationship of helix length to bilayer thickness and by the cholesterol concentration, *Biochemistry 36*, 10213−10220.
10. Clark, E. H., East, J. M., and Lee, A. G. (2003) The role of tryptophan residues in an integral membrane protein: diacylglycerol kinase, *Biochemistry 42*, 11065−11073.
11. Monks, S. A., Needleman, D. J., and Miller, C. (1999) Helical structure and packing orientation of the S2 segment in the *Shaker* K^+ channel, *J. Gen. Physiol. 113*, 415−423.
12. Hong, K. H., and Miller, C. (2000) The lipid-protein interface of a Shaker K^+ channel, *J. Gen. Physiol. 115*, 51−58.
13. Zhou, Y. F., Wen, J., and Bowie, J. U. (1997) A passive transmembrane helix, *Nat. Struct. Biol. 4*, 986−990.
14. Nagy, J. K., and Sanders, C. R. (2004) Destabilizing mutations promote membrane protein misfolding, *Biochemistry 43*, 19−25.
15. Chattopadhyay, A., and London, E. (1987) Parallax method for direct measurements of membrane penetration depth utilizing fluorescence quenching by spin-labeled phospholipids, *Biochemistry 26*, 39−45.
16. Perozo, E., Cortes, D. M., Sompornpisut, P., and Martinac, B. (2002) Open channel structure of MscL and the gating mechanism of mechanosensitive channels, *Nature 418*, 942−948.
17. Chang, G., Spencer, R. H., Lee, A. T., Barclay, M. T., and Rees, D. C. (1998) Structure of the MscL homolog from Mycobacterium tuberculosis: A gated mechanosensitive ion channel, *Science 282*, 2220−2226.
18. Powl, A. M., East, J. M., and Lee, A. G. (2003) Lipid−protein interactions studied by introduction of a tryptophan residue: the mechanosensitive channel MscL, *Biochemistry 42*, 14306−14317.
19. Sukharev, S. I., Sigurdson, W. J., Kung, C., and Sachs, F. (1999) Energetic and spatial parameters for gating of the bacterial large conductance mechanosensitive channel, MscL, *J. Gen. Physiol. 113*, 525−539.
20. Hamill, O. P., and Martinac, B. (2001) Molecular basis of mechanotransduction in living cells, *Physiol. Rev. 81*, 685−740.
21. Perozo, E., Kloda, A., Cortes, D. M., and Martinac, B. (2002) Physical principles underlying the transduction of bilayer deformation forces during mechanosensitive channel gating, *Nat. Struct. Biol. 9*, 696−703.
22. Levina, N., Totemeyer, S., Stokes, N. R., Louis, P., Jones, M. A., and Booth, I. R. (1999) Protection of *Escherichia coli* cells against extreme turgor by activation of MscS and MscL mechanosensitive channels: identification of genes required for MscS activity, *EMBO J. 18*, 1730−1737.
23. Yoshimura, K., Batiza, A., Schroeder, M., Blount, P., and Kung, C. (1999) Hydrophilicity of a single residue within MscL correlates with increased channel mechanosensitivity, *Biophys. J. 77*, 1960−1972.
24. East, J. M., and Lee, A. G. (1982) Lipid selectivity of the calcium and magnesium ion dependent adenosinetriphosphatase, studied with fluorescence quenching by a brominated phospholipid, *Biochemistry 21*, 4144−4151.
25. Warren, G. B., Toon, P. A., Birdsall, N. J. M., Lee, A. G., and Metcalfe, J. C. (1974) Reversible lipid titrations of the activity of pure adenosine triphosphatase-lipid complexes, *Biochemistry 13*, 5501−5507.
26. Ladokhin, A. S., Jayasinghe, S., and White, S. H. (2000) How to measure and analyze tryptophan fluorescence in membrane properly, and why bother?, *Anal. Biochem. 285*, 235−245.

27. Chen, R. F. (1967) Fluorescence quantum yields of tryptophan and tyrosine, *Anal. Lett. 1*, 35−42.
28. Maurer, J. A., and Dougherty, D. A. (2003) Generation and evaluation of a large mutational library from the *Escherichia coli* mechanosensitive channel of large conductance, MscL—Implications for channel gating and evolutionary design, *J. Biol. Chem. 278*, 21076−21082.
29. Bolen, E. J., and Holloway, P. W. (1990) Quenching of tryptophan fluorescence by brominated phospholipid, *Biochemistry 29*, 9638−9643.
30. Ladokhin, A. S. (1999) Analysis of protein and peptide penetration into membranes by depth-dependent fluorescence quenching: Theoretical considerations, *Biophys. J. 76*, 946−955.
31. Caputo, G. A., and London, E. (2003) Using a novel dual fluorescence quenching assay for measurement of tryptophan depth within lipid bilayers to determine hydrophobic α-helix locations within membranes, *Biochemistry 42*, 3265−3274.
32. Perochon, E., Lopez, A., and Tocanne, J. F. (1992) Polarity of lipid bilayers. A fluorescence investigation, *Biochemistry 31*, 7672−7682.
33. Ghiggino, K. P., Lee, A. G., Meech, S. R., O'Connor, D. V., and Phillips, D. (1981) Time-resolved emission spectroscopy of the dansyl fluorescence probe, *Biochemistry 20*, 5381−5389.
34. Perozo, E., Kloda, A., Cortes, D. M., and Martinac, B. (2001) Site-directed spin-labeling analysis of reconstituted MscL in the closed state, *J. Gen. Physiol. 118*, 193−205.
35. Elmore, D. E., and Dougherty, D. A. (2003) Investigating lipid composition effects on the mechanosensitive channel of large conductance (MscL) using molecular dynamics simulations, *Biophys. J. 85*, 1512−1524.
36. Lee, A. G. (2004) How lipids affect the activities of integral membrane proteins, *Biochim. Biophys. Acta 1666*, 62−87.
37. Esnouf, R. M. (1999) Further additions to MolScript version 1.4, including reading and contouring of electron-density maps, *Acta Crystallogr., Sect. D 55*, 938−940.
38. Akerlof, G., and Short, O. A. (1936) The dielectric constant of dioxane-water mixtures between 0 and 80°, *J. Am. Chem. Soc. 58*, 1241−1243.

BI047338G